Technology Reports (Special Articles) 5G Evolution Millimeter Wave Field Experiments

Special Articles on 5G (2)—NTT DOCOMO 5G Initiatives for Solving Social Problems and Achieving Social Transformation—

Field Experiments on Millimeter-wave Radio Technology for 5G Evolution

6G Laboratories Yoshihisa Kishiyama Daisuke Kitayama Satoshi Suyama Yuki Hokazono

As commercial 5G deployment has already begun around the world, R&D for 5G evolution to further develop 5G in the 2020s is required. In this article, we describe efforts with three field experiments related to further evolution of 5G millimeter-wave radio technology, an important issue in 5G evolution.

1. Introduction

5th generation mobile communications systems (5G) have already gone into commercial operation around the world, and NTT DOCOMO also launched commercial services in March 2020. However, as challenges and further expectations for 5G are identified, research and development to further 5G technological development will be required into the 2020s. NTT DOCOMO began examining requirements for 5G evolution and 6G from around 2017 [1], and released 6G technical concepts (a white paper) in January 2020 [2]. A number of initiatives are also underway regarding field experiments for 5G evolution.

This article describes field experiments using the 28 GHz band, a 5G frequency band, as part of efforts to further develop millimeter-wave*1 radio technology, a crucial issue in 5G evolution. Specifically, we describe a coverage improvement experiment with a metasurface*2 reflector [3] [4], a 5G high-speed travel experiment on the Tokaido Shinkansen [5] [6], and a field experiment of fishing area remote monitoring using an underwater drone [7] [8].

*1 Millimeter-wave: Customarily called "Millimeter waves", these are radio signals in the frequency band from 30 GHz to 300 GHz as well as the 28 GHz band targeted for 5G.

2. Coverage Improvement Experiment with a Metasurface Reflector

With millimeter waves, the challenge is covering areas in the shadows of shield objects such as buildings or trees that put the Base Station (BS) antenna and the Mobile Station (MS) out of radio sight (non-line-of-sight) of each other. To improve coverage in such non-line-of-sight environments and communications quality, metamaterial*3 and metasurface technologies composed by regular positioning of structures smaller than the wavelength have recently been gaining attention [9]. Applying these technologies to a reflector makes it possible to freely design the propagation direction and beamwidth*4 of reflected waves regardless of the installation direction/size of the reflector. Thus, this technology can be installed on a wall surface of a building, etc., to guide reflected waves in a specific direction. We performed field experiments of the technology in a real environment.

2.1 Experiment Overview

In this experiment, a 28 GHz band 5G transmission experimental apparatus fitted with the same BS (made by Ericsson) and MS (made by Intel) beamforming*5 as in literature [10] was used. The effective bandwidth per Component Carrier (CC)*6 was 90 MHz, with 4CC Carrier Aggregation (CA)*7 performed from 27.5 GHz to 27.9 GHz. The time ratio of the Up Link (UL) and Down Link (DL) subframes*8 was 1:1.

Figure 1 shows the concept of the metasurface reflector and the metasurface reflector used in this experiment. Metawave Corporation manufactured the metasurface reflector. The unit cell*9 structure of the metasurface is patterned with patch-type metal on a substrate surface, and the rear surface is covered with metal. The structure of the metal patches and the rear metal determines the resonance frequency, and the phase of the reflected waves varies greatly around this resonance frequency. Accordingly, any reflected wavefront can be designed by distributing the patch size within

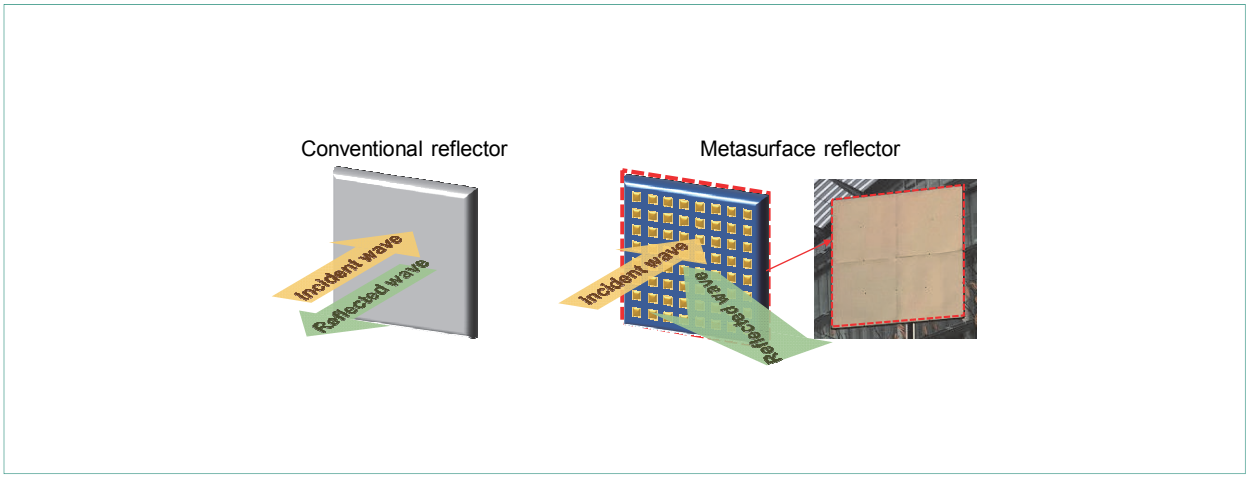

Figure 1 Conceptual diagram of a conventional reflector and the metasurface reflector used in this experiment

*2 Metasurface: An artificial surface technology with two-dimensional periodic arrangement of structures that is a type of artificial medium (metamaterial (see *3)), and that achieves an arbitrary dielectric constant and magnetic permeability by periodic arrangement of structures that are smaller than the wavelength.

*3 Metamaterial: An artificial material that causes electromagnetic waves to behave in ways that they do not in natural materials.

*4 Beamwidth: The antenna radiation angle at which the beam is radiated with gain of –3dB or less from the maximum antenna gain.

*5 Beamforming: A technique for increasing or decreasing the gain of multiple antennas in a specific direction by controlling the phase of the antennas to form a directional pattern of the antennas.

the substrate to cover the area.

The experimental environment and the angles of incidence/reflection designed for the metasurface reflectors are shown in **Figure 2**. Experiments were performed by installing a BS antenna on the rooftop (at a height of 37.4 m) of the Tokyo International Exchange Center in the Odaiba area of Tokyo. Since the road in front of the building was shielded by the installation building itself and communications quality was poor, we installed a metasurface reflector at a position in line of sight of the BS, and verified that the reflected waves from the metasurface reflector created a 5G coverage area in the road front of the building. The metasurface reflector used in this verification test was designed to have incidence/reflection angles in the vertical direction of approximately 50°/30° and was installed at a height of 3.4 m. To form a reflected wave with sufficient power, the size of the reflective plate was 80 cm x 80 cm. However, assuming that the incident wave is a planar wave*10, only a very narrow beam (half power beamwidth*11: approximately 2° to 3°) is formed in the open area and thus the area covered thins. Therefore, the metasurface reflector was designed so that both the reflected angle and the half power beamwidth of the reflected wave are 18°.

2.2 Experimental Results

Distributions of received power (Beam Reference Signal Received Power (BRSRP)*12) and DL throughput characteristics measured by driving the MS vehicle in front of the International Exchange Center are shown in **Figure 3**. Without the metasurface reflector installed, the BRSRP went below −70 decibels milli (dBm)*13 because the front of the building is non-line-of-sight, resulting in a significant drop in received power compared to the area in radio sight (> −50 dBm). However, with the metasurface reflector installed, it can be seen that BRSRP and throughput characteristics improve due to the 28 GHz band reflected waves

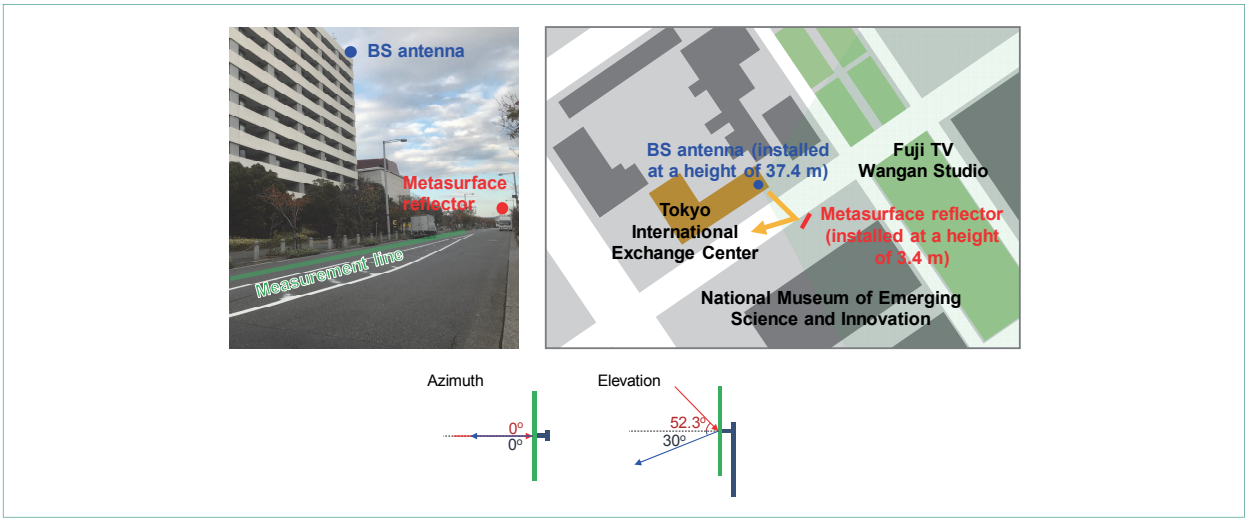

Figure 2 Metasurface reflector experimental environment and angle of incidence/reflection design of the reflector

*6 CC: A term used in CA (see *7) to denote one of several frequency blocks.
*7 CA: A technology that enables high-speed communications by bundling multiple blocks of frequencies to create a wide-bandwidth.
*8 Subframe: A unit of radio resources in the time domain consisting of multiple Orthogonal Frequency Division Multiplexing (OFDM) symbols.
*9 Cell: The unit of area division that make up the service area of a mobile communications network.
*10 Planar wave: An electromagnetic wave where the amplitude and phase of the electromagnetic field are constant within a plane perpendicular to the propagation direction.
*11 Half power beamwidth: The angular range over which the power emitted from an antenna goes from its maximum value to half of that value. Expresses the sharpness of the directivity.

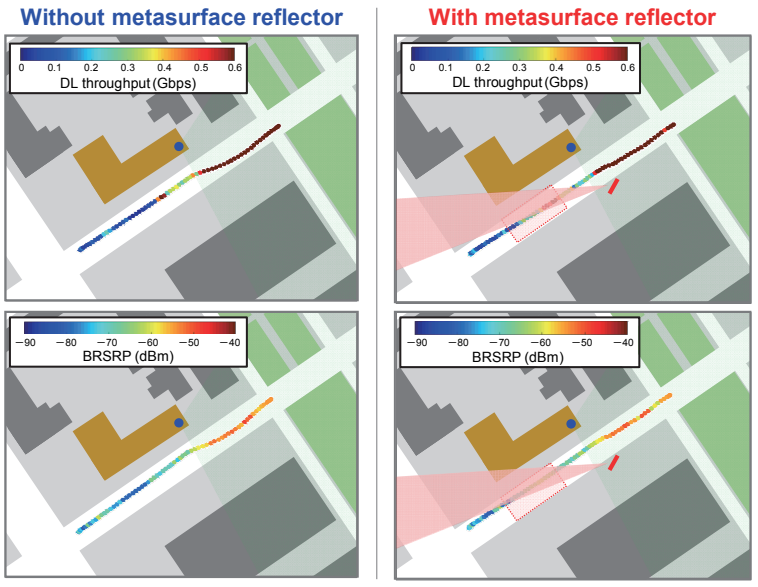

Figure 3 Distributions of received power and DL throughput

reaching the front of the building.

The variation characteristics of BRSRP and DL throughput relative to the travel distance of the MS vehicle are shown in **Figure 4**. The installation of the metasurface reflector improved BRSRP over a driving distance range of 40 m to 75 m corresponding to the front area of the building, confirming an improvement of up to approximately 15 dB. The throughput was also improved in the same range to a maximum of approximately 500 Mbps (no reflector plate: 60 Mbps --> with reflector plate: 560 Mbps).

3. 5G High-mobility Experiment Using the Tokaido Shinkansen

For 5G evolution, NTT DOCOMO is examining how high-speed communications using high-frequency bands such as 28 GHz can be provided stably even in high-speed mobile environments such as high-speed trains. Doppler frequency shifts[*14] are higher in high-frequency bands than in low-frequency bands, and in high-speed train environments such as the Shinkansen, since Doppler frequency shifts are further increased with high mobility, there are concerns about deterioration in characteristics. Addressing these issues, in cooperation with Central Japan Railway Company, we conducted transmission experiments from August to September 2019 near Shin-Fuji Station in Shizuoka Prefecture using a 28 GHz-band 5G experimental device with a beam tracking function and the test version of an N700S-model Shinkansen rolling stock traveling at 283 km/h on the Tokaido Shinkansen railway.

*12 BRSRP: RSRP per beam. RSRP is the reception level of a reference signal measured at the mobile terminal.

*13 dBm: Power value [mW] expressed as 10 log (P). The value relative to a 1 mW standard (1 mW = 0 dBm).

*14 Doppler frequency shift: The shift in carrier frequency due to the Doppler effect.

3.1 Experiment Overview

In the experiment, three BSs for 5G experiment were installed on the road along the Tokaido Shinkansen railway, approximately 100 m away from the railway. A detailed diagram of the setup is shown in **Figure 5**. The MS was placed near the window glass by a passenger seat in the test version of the N700S-model Shinkansen rolling stock. Between BS2 and BS3, there are trees and a river at approximately 1,000 to 1,100 m points creating a non-line-

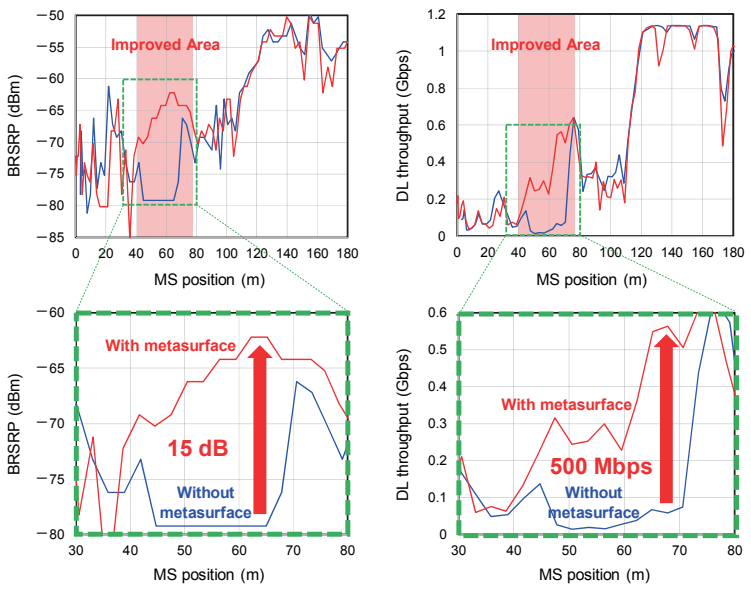

Figure 4 Variable characteristics of received power and DL throughput

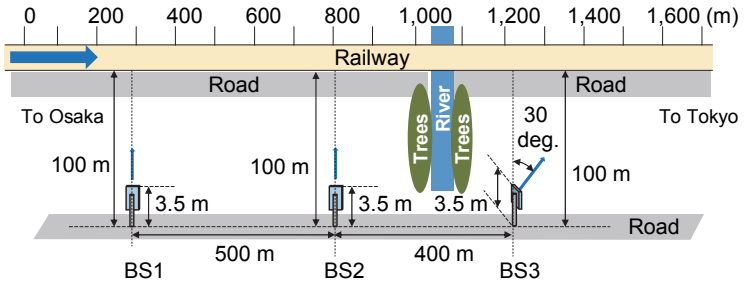

Figure 5 BS positioning

of-sight environment that the MS would traverse. The bandwidth of the 28 GHz-band 5G experimental equipment is 700 MHz and the maximum DL data rate is 3.3 Gbps. Each BS is equipped with two 48-element array antennas*15 and the MS is equipped with two 32-element array antennas, each generating a beam. To maximize received power, combinations of BS and MS beam candidates are selected every 10 ms to achieve beam tracking.

3.2 Experimental Results

Figure 6 shows the DL throughput performances measured during a single run. The throughput was measured at a point approximately 180 m, achieving up to approximately 320 Mbps in front of BS1. A throughput of up to approximately 170 Mbps was observed at BS2, a throughput of up to 980 Mbps was measured in the frontal direction of BS3, and 50 to 200 Mbps was observed up to the 1,700 m point. The Cumulative Distribution Function (CDF)*16 properties of DL throughput by MS moving speed obtained in multiple run experiments are shown in **Figure 7**. The throughput at the MS moving speed of 0 to 20 km/h is the result of driving a car on the road parallel to the Tokaido Shinkansen railway. The throughput deteriorated as the MS moved faster, which is likely due to an increase in Doppler frequency shift. The median value*17 of the throughput at 283 km/h was approximately 130 Mbps and the maximum value was 1.3 Gbps. We confirmed that communication exceeding 1 Gbps can be obtained using the 28 GHz band, if beam tracking can be performed in high-speed train environments.

4. Field Experiment of Remote Monitoring of Fishing Grounds Utilizing an Underwater Drone

One challenge for 5G evolution and 6G is coverage

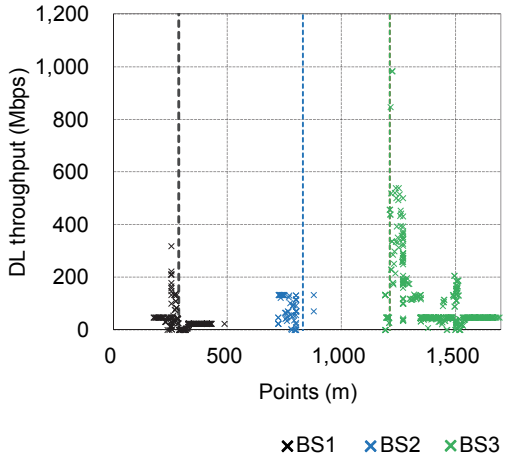

Figure 6 DL throughput performances

*15 Array antenna: An antenna consisting of multiple elements.
*16 CDF: A function that represents the probability that a random variable will take on a value less than or equal to a certain value.
*17 Median value: The value in the middle when countable data is ordered in increasing (or decreasing) size.

expansion in the sky, sea and space [2]. Such initiatives can be expected to further expand the environments in which people and objects can operate and thus create new industries. As an example of the "sea" use case, in collaboration with the University of Tokyo, NTT DOCOMO conducted a field experiment of remote monitoring of fishing grounds utilizing a 5G-enabled underwater drone [11].

4.1 Experiment Overview

Figure 8 shows the experimental structure. An MS was installed on a small vessel moored at sea, and an underwater drone wired to the MS device was put into the sea where an oyster farm is located. Full HD underwater video captured by underwater drone camera was transmitted by radio with UL to a shore-based BS, while at the same time pilot signals were sent to the underwater drone by radio with DL from BS to MS without

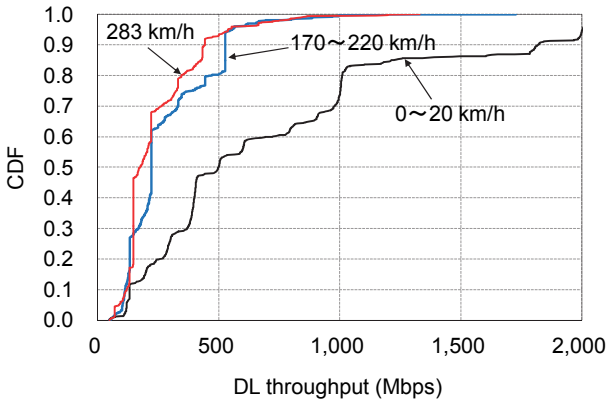

Figure 7 CDF of DL throughput by MS moving speed

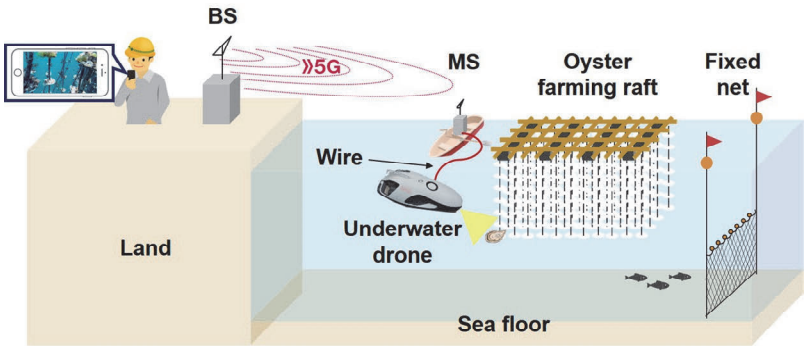

Figure 8 Experimental configuration of remote monitoring of fishing ground

any time lag. The vessel was moored approximately 150 m from the BS at the location of the oyster farm rafts. In this experiment, the same 28 GHz band 5G transmission experimental equipment used in the experiment described in Section 2 was used.

The experiment was conducted at Yanagawa Fisheries, Etajima City, Hiroshima Prefecture. Taken from on land, **Photo 1** shows the BS installed on land and the MS installed on the vessel. At the time of the experiment, the height of the land from the sea surface was approximately 3.0 m, the antenna height of the BS was approximately 1.7 m, and the mechanical tilt[*18] was set at 0°. **Photo 2** shows the MS taken onboard the vessel. The approximately 1.0 m antenna height of the MS was adjusted to approximately 2.0 m from sea level. The underwater drone used was a PowerRay [12] from PowerVision Japan Co., Ltd.

4.2 Experimental Results

In this experiment, the target BLock Error Rate (BLER)[*19] was set to both 0.1% (a focus on stability) and 10% (a focus on communications speed) to evaluate considering the trade-off between communication speed and stability in 5G industrial usage. The CDF characteristics of the DL throughput are shown in **Figure 9** (a), and the CDF of the DL Modulation and Coding Scheme (MCS)[*20] is

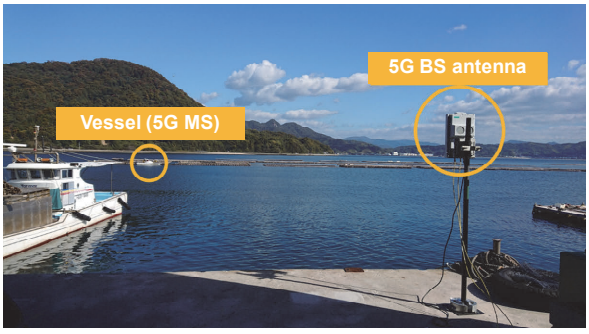

Photo 1 5G BS installed on land and 5G MS installed on the vessel

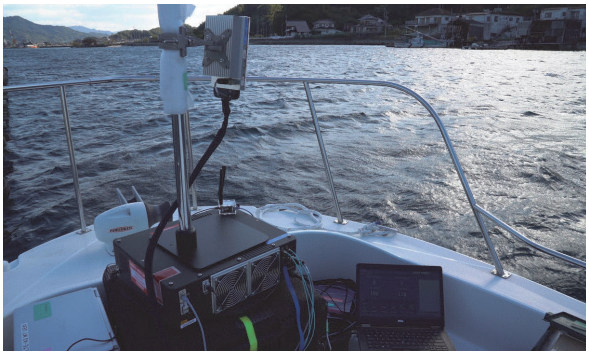

Photo 2 5G MS on deck

*18 Tilt: The inclination of an antenna's main beam direction in the vertical plane.

*19 BLER: The error rate in blocks of transmitted data.

*20 MCS: Combinations of modulation scheme and coding rate decided on beforehand when performing Adaptive Modulation and Coding (AMC).

shown in Fig. 9 (b). From the figure, it can be seen that the variation in DL throughput is smaller when the target BLER is fixed to 0.1%. This is because the MCS is held low to suppress information errors due to the rocking of the vessel. In contrast, with the target BLER at 10%, a relatively high MCS is easy to select and a better throughput is obtained. Since communication speeds in the order of only a few percent of DL throughput characteristics is needed for the small capacity data transmission required to control the underwater drone, it is generally preferable to lower the target BLER to prioritize stability of communications. However, in the case of this experiment, packet loss*21 was not caused by retransmission even with a target BLER of 10%, making low-latency drone control sufficiently possible.

Figure 10 (a) shows the CDF characteristics of

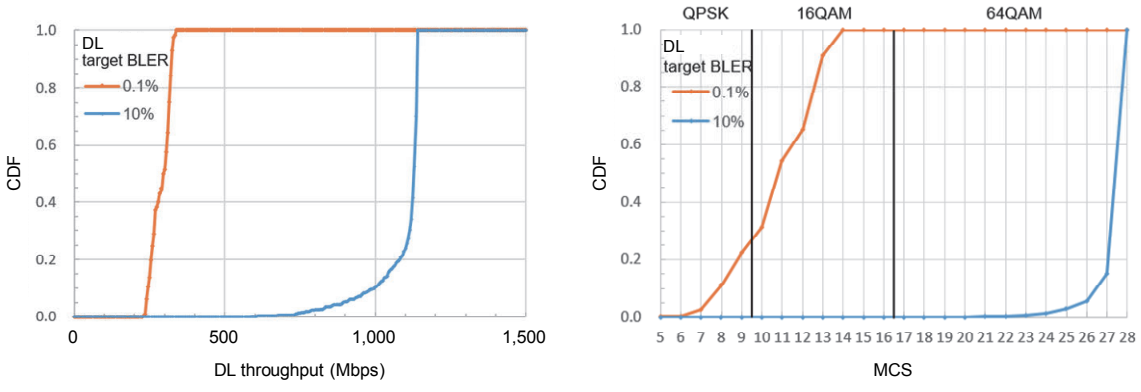

Figure 9 DL CDF characteristics per target BLER

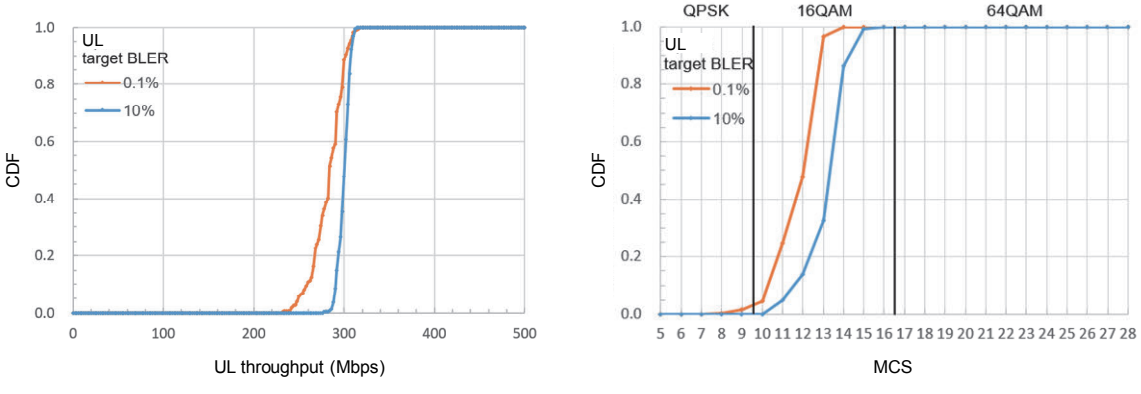

Figure 10 UL CDF characteristics per target BLER

*21 Packet loss: The failure of error-free data packets to be delivered to their destination due to congestion or other issues.

UL throughput when the target BLER is set to 0.1% and 10%, and Fig. 10 (b) shows the CDF of the UL MCS. From the figure, although there was no significant difference in UL throughput variation when the target BLER was set to 0.1% and 10%, slightly higher throughput was obtained when the target BLER was 10%. Compared to DL, the reason there is no difference is likely due to insufficient Signal-to-Noise Ratio (SNR)*22 for selecting a high UL MCS with this experimental configuration and equipment.

Figure 11 shows video of the oyster farm captured by the underwater drone when the target BLER for UL and DL was set to 10%. The user was able to operate the underwater drone without time lag while viewing the underwater scene in high resolution through full HD video.

5. Conclusion

This article has described field experiments using the 28 GHz band, a 5G frequency band, as part of efforts to further develop millimeter wave technology, a crucial issue in 5G evolution. We described a coverage improvement experiment with a metasurface reflector, a 5G high-speed travel experiment on the Tokaido Shinkansen, and a field experiment of fishing ground remote monitoring using an underwater drone. Moving forward with 5G evolution, the expansion of non-terrestrial coverage, and Ultra-Reliable and Low-Latency Communications (URLLC) capabilities for industry will be considered in standardization. NTT DOCOMO plans to continue to work on evolving these radio technologies.

REFERENCES

[1] Y. Kishiyama: "Initial review of Beyond 5G radio access technology," IEICE BS-2-2, Sep. 2017 (In Japanese).
[2] NTT DOCOMO: "White Paper: 5G Evolution and 6G," Jan. 2020.
[3] NTT DOCOMO Press Release: "World's first successful demonstration experiment for enlarging a 5G area in the 28 GHz band with a reflector using metamaterial technology," Dec. 2018 (In Japanese).
[4] D. Kitayama, D. Kurita, K. Miyachi, Y. Kishiyama, S.

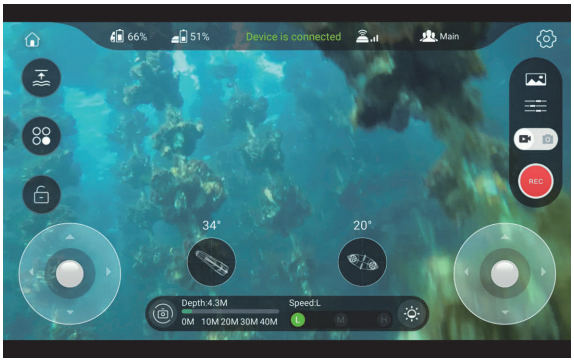

Figure 11 Oyster farm video transmitted in 5G

*22 SNR: The ratio of the desired signal power to the noise power.

Itoh and T. Tachizawa: "5G Radio Access Experiments on Coverage Expansion Using Metasurface Reflector at 28 GHz," 2019 IEEE Asia-Pacific Microwave Conference (APMC), pp.435-437, 2019.

[5] NTT DOCOMO Press Release: "DOCOMO Achieves World's First 5G Communication Between High-speed Bullet Train and Experimental Base Stations," Sep. 2019.

[6] N. Nonaka, K. Muraoka, T. Okuyama, S. Suyama, Y. Okumura, T. Asai and Y. Matsumura: "28 GHz band 5G transmission experiments in high-speed mobile environments using the Shinkansen," Information Technology Bulletin, RCS 2019-264, Dec. 2019 (In Japanese).

[7] NTT DOCOMO Press Release: "Successful demonstration experiments for remote monitoring of fishing grounds utilizing 5G and an underwater drone," Nov. 2019 (In Japanese).

[8] Y. Hokazono, T. Minamida, Y. Aburakawa, D. Ping and A. Nakao: "Underwater drone remote control experiments using the 28 GHz band in 5G," IEICE Technical Report, NS 2019-241, Mar. 2020 (In Japanese).

[9] M. D. Renzo, M. Debbah, D. Phan-Huy, A. Zappone, M. Alouini, C. Yuen, V. Sciancalepore, G. C. Alexandropoulos, J. Hoydis, H. Gacanin, J. Rosny, A. Bounceur, G. Lerosey and M. Fink: "Smart radio environments empowered by reconfigurable AI meta-surfaces: an idea whose time has come," EURASIP Journal on Wireless Commun. and Networking 2019, No.129, May 2019.

[10] D. Kurita, K. Tateishi, D. Kitayama, A. Harada, Y. Kishiyama, H. Murai, S. Itoh, A. Simonsson, and P. Okvist: "Indoor and Field Experiments on 5G Radio Access for 28-GHz Band Using Distributed MIMO and Beamforming," IEICE Trans. Commun., Vol.E102-B, No.8, Aug. 2019.

[11] A. Nakao: "Regional Revitalization through DX – Utilization of Latest Information and Communication Technology," NTT DOCOMO Technical Journal, Vol.28, No.2, pp.4-7, Jul. 2020 (In Japanese).

[12] PowerVision Japan Co., Ltd. "PowerRay," (In Japanese). https://www.powervision.me/jp/product/powerray (available Aug. 2020).